Biol. Cybern. 69, 87–95 (1993)

Biological Cybernetics

A basic biophysical model for bursting neurons

Evyatar Av-Ron [1], Hanna Parnas [2], Lee A. Segel [1]

[1] Department of Applied Mathematics and Computer Science, Weizmann Institute of Science, Rehovot 76100, Israel
[2] Department of Neurobiology, Institute of Life Sciences, Hebrew University, Jerusalem 91904, Israel

Received: 29 November 1991/Accepted in revised form: 30 November 1992

Abstract. Presented here is a basic biophysical cell model for bursting, an extension of our previous model (Av-Ron et al. 1991) for excitability and oscillations. By changing a limited set of model parameters, one can describe different patterns of bursting behavior in terms of the burst cycle, the durations of oscillation and quiescence, and firing frequency.

1 Introduction

This is a second paper in a series aimed at constructing canonical models for neurons that exhibit different firing patterns. More precisely, as stated in the first paper of the series (Av-Ron et al. 1991, hereafter referred to as paper I), we aim to show that a common biophysical cellular model, but with different parameter values, can exhibit different observed cellular behaviors. (By biophysical model we mean a model where every variable or process can be associated with a biophysical mechanism.) In subsequent publications our model neuron cells will be used to simulate, and to gain an understanding of, the behavior of small neuronal networks. To this end, for reasons discussed in paper I, we have chosen to focus on the cardiac ganglion of the lobster.

In paper I we presented a minimal cellular model that exhibits excitability and oscillatory behavior. Furthermore, by analyzing the effects of parameter variation, we ascertained the main biophysical processes that (according to our model) determine whether a cell is an oscillatory or an excitable cell.

However, neurons not only show oscillation or excitability. In addition "burster" neurons exhibit intervals of high frequency oscillations, which alternate with periods of quiescence. An example of such a behavior is shown in Fig. 1, which depicts typical behavior of the neurons of the lobster cardiac ganglion (Bullock and Terzuolo 1957). To obtain bursting behavior, we must extend the minimal model of paper I.

A number of authors have considered bursting models; for reviews see Rinzel and Lee (1987) and Rinzel and Ermentrout (1989). Our approach supplements earlier work mainly because of its focus on striving to explain a variety of observed cellular behaviors with a single model and its efforts to keep the basic model as simple as possible. Hence, our strategy in constructing the basic model for bursting is to base it on the minimal model of paper I. We then will choose, from several possible biophysical mechanisms that seem capable of turning an oscillator into a burster, those that seem most justified for the cardiac ganglion of the

Correspondence to: E. Av-Ron, Groupe de Bioinformatique, URA 686 – Ecole Normale Superieure, 46 rue D'Ulm, F-75320 Paris Cedex 05, France

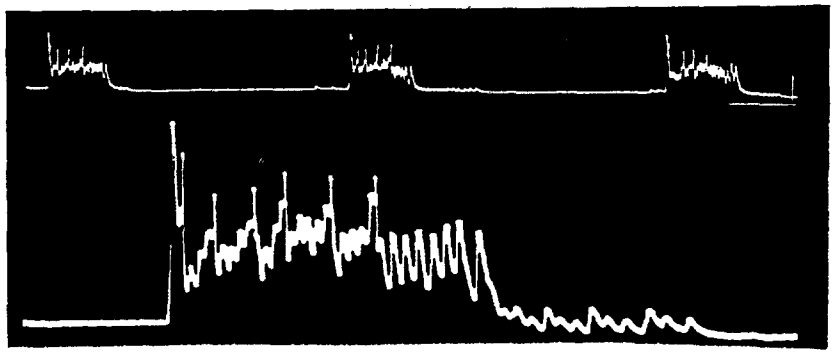

Fig. 1. a Intracellular voltage recording from a large cell of the cardiac ganglion of the lobster *Panulirus interruptus*. **b** Enlargement. Scales in **a** (*right*): 10 mV, 500 ms. Taken with permission from Bullock and Terzuolo (1957)

lobster. We will determine which of the biophysical parameters are mainly responsible for variation in the neurobiologically significant burst properties, that is the frequency of firing within the burst, the duration of the firing period (oscillation) and the interval between the firing periods (quiescence).

In a third paper we will apply the conclusions obtained in this paper to model the neurons of the lobster cardiac ganglion.

2 A minimal cell model

The minimal cell model of paper I is based on the work of Hodgkin and Huxley (1952) and Rinzel (1984). The model involves three types of current: an inward sodium current I_{Na}, an outward potassium current I_K and a leak current I_L. An ion current I_i can be described by the product of its maximal conductance $\bar{g}_i$, of activation and inactivation variables, and of the driving force $(V - V_i)$. The system is represented by two variables, the voltage variable V and a recovery variable W. W is called a recovery variable because it is a linear combination of the two Hodgkin–Huxley variables h and n that are responsible for ending the action potential and returning the membrane to its resting potential. As was shown in paper I, the use of W – which dates from FitzHugh (1961) – reduces the number of variables in the model, allowing for simpler mathematical analysis (phase plane and stability), while not significantly altering the model dynamics.

The minimal model of paper I is composed of two differential equations:

$$C_m \frac{dV}{dt} = I - I_{Na} - I_K - I_L, \qquad \frac{dW}{dt} = \frac{W_\infty(V) - W}{\tau_w(V)}. \tag{1, 2}$$

The current-voltage equations are

$$I_{Na} = \bar{g}_{Na} m_\infty^3(V)(1 - W)(V - V_{Na}) \tag{3a}$$

$$I_K = \bar{g}_K (W/s)^4 (V - V_K), \qquad I_L = \bar{g}_L (V - V_L) \tag{3b, c}$$

The following equations give the voltage dependence of the steady-state recovery (W_∞), the steady-state sodium activation (m_∞) and the relaxation time for recovery (τ_w):

$$W_\infty(V) = (1 + \exp[-2a^{(w)}(V - V_{1/2}^{(w)})])^{-1} \tag{4}$$

$$m_\infty(V) = (1 + \exp[-2a^{(m)}(V - V_{1/2}^{(m)})])^{-1} \tag{5}$$

$$\tau_w(V) = (\bar{\lambda} \exp[a^{(w)}(V - V_{1/2}^{(w)})] + \bar{\lambda} \exp[-a^{(w)}(V - V_{1/2}^{(w)})])^{-1} \tag{6}$$

The steady-state functions of (4) and (5) are modeled as sigmoid curves. The parameter $V_{1/2}$ is the voltage for the half-maximal value and the parameter a controls the slope of the curve at this midpoint (inflection point). For further detail see paper I.

The model, (1)–(6), can exhibit excitability, in that a suprathreshold stimulus will cause it to generate an action potential. For other parameter regimes the model yields oscillatory behavior.

2.1 The minimal model adjusted to the lobster cardiac neurons

In paper I we showed the visual fit of the minimal cell model to the lobster giant axon action potential. As our long-term goal is to model the lobster cardiac ganglion, we choose here parameters that yield agreement with existing data concerning the lobster cardiac neurons. Compared to the giant axon, the cardiac ganglion neurons have a higher resting potential (between −50 and −60 mV) (Bullock and Terzuolo 1957) and a lower threshold (between 1.3 and 11 mV) (Otani and Bullock 1959). There are no voltage clamp data on the cardiac nerve cell axons, so that there are numerous ways to achieve a model with these constraints. To select among them, we arranged that there be a reasonable fit to observations of the I-V curves of lobster giant axon, as it is known that I-V curves tend to be quite similar among various cell types (Hille 1992). An action potential that results when the parameters fitting the lobster cardiac neuron (1)–(6) are employed is presented in Fig. 2.

3 A minimal bursting model

The qualitative behavior of the minimal model (1)–(6) depends on the parameter values. Three relevant behaviors can be found: (i) There is a globally stable steady state, i.e. no matter what the initial conditions are, as time goes on all solutions approach closer and closer to the steady state. (ii) There is a globally stable limit cycle, i.e. with time, all solutions tend toward a particular well-defined oscillation. (iii) Bistability exists in the form of two (locally) stable states, a steady state and an oscillation. Bistability is illustrated in Fig. 3. The

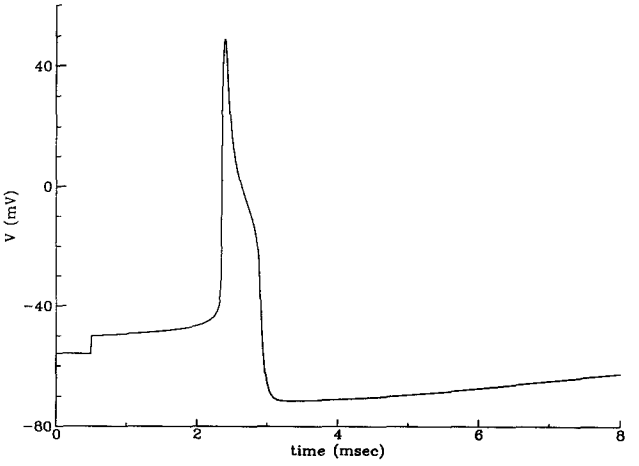

Fig. 2. A single action potential of the minimal lobster cardiac model (1)–(6). The action potential is triggered by raising the membrane potential past threshold, to −50 mV, at $t = 0.5$ ms. The resting potential is −56 mV. Model parameters: $V_{1/2}^{(m)} = -31$ mV, $a^{(m)} = 0.065$, $V_{1/2}^{(w)} = -46$ mV, $a^{(w)} = 0.055$, $\bar{\lambda} = 0.08$, $s = 1$. All other parameters take the Hodgkin and Huxley (1952) values (with $V = V_{HH} - 60$): $C_m = 1\ \mu$F/cm^2, $\bar{g}_{Na} = 120$ mS/cm^2, $\bar{g}_K = 36$ mS/cm^2, $\bar{g}_L = 0.3$ mS/cm^2, $V_{Na} = 55$ mV, $V_K = -72$ mV, $V_L = -50$ mV. (Note Hodgkin-Huxley $V_L = -49.4$ mV)

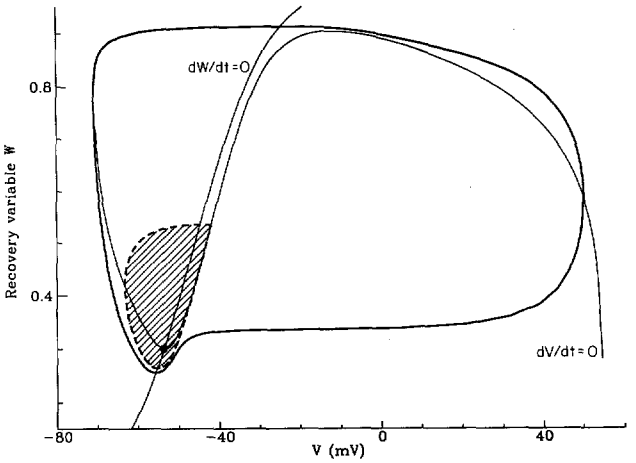

Fig. 3. Bistability of the minimal lobster cardiac model. Nullclines for (1) and (2) with corresponding stable steady-state point (*heavy dot*) and stable limit cycle (*solid line*) traversed counterclockwise. Unstable limit cycle (*dashed line*) bounds shaded domain of attraction of steady-state point. Parameters as in Fig. 2 except that $\bar{g}_K = 15$ mS/cm^2

shaded area of this figure corresponds to the domain of attraction of the steady state, namely the set of initial conditions starting from which solutions tend to the steady state. The unshaded area corresponds to the domain of attraction of the limit cycle oscillation.

For definiteness, let us consider what qualitative behaviors are possible for a range of values of the maximal potassium conductance $\bar{g}_K$. These behaviors are evident from the so-called bifurcation diagram of Fig. 4a. From left to right, there is a parameter domain where the steady state is globally stable, then (for $1.3 < \bar{g}_K < 3$) a region of bistability, then a region with a globally stable limit cycle, then another region of bistability, and finally (for $\bar{g}_K > 16$) another region where the steady state is a global attractor.

In overall terms, bursting can be obtained by supplementing the minimal model by a process that shifts a parameter such as $\bar{g}_K$ in a cyclic manner back and forth between a region associated with oscillations and a region associated with a steady state. Suppose that this process is slow compared to the changes described by the minimal model. Then the qualitative results for the minimal model should remain valid, so that the system will switch back and forth between virtual quiescence and oscillation, as is observed in bursting. It turns out that a parameter region exhibiting bistability is important if one is to obtain a minimal burster model. This point will be discussed further below.

3.1 Minimal bursters

The question now arises of what should be the "control parameter" whose alteration produces bursting. In paper I we found that the most natural parameter to alter the model dynamics is the maximal conductances of the different ions, i.e. $\bar{g}_{NA}$, $\bar{g}_K$ and $\bar{g}_L$. Altering the conductances was therefore a "natural" thing to do because they have a strong effect on model dynamics

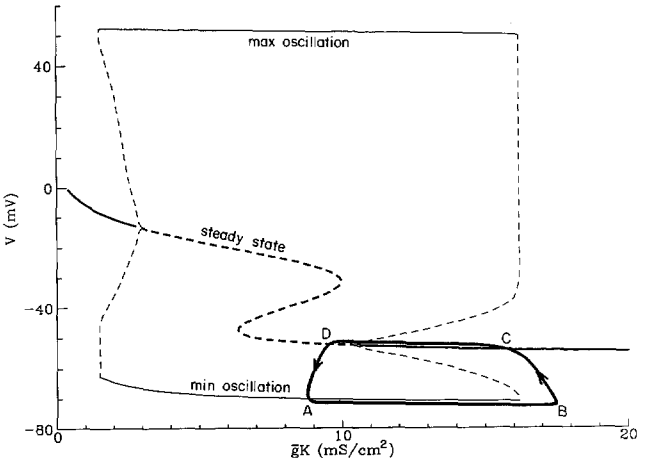

a

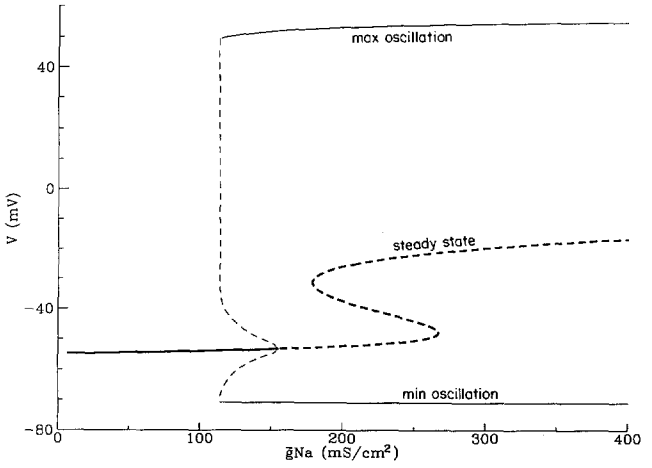

b

Fig. 4. a Bifurcation diagram as a function of $\bar{g}_K$, the maximal potassium conductance per unit area. **b** Bifurcation diagram as a function of $\bar{g}_{Na}$, the maximal sodium conductance per unit area. Depicted are steady states that are stable (*heavy solid line*) and unstable (*heavy dashed line*) as well as minimum and maximum voltages for limit cycle solutions, both stable (*light solid line*) and unstable (*light dashed line*). The *dark closed curve* schematically corresponds to the course of a burst (see text). Fixed parameters as in Fig. 2.

and can be modified by biophysically plausible mechanisms. It was these parameters that we concentrated on as a basis for bursting.

As an aid to choosing suitable modifications of the conductances, in Fig. 4 we present bifurcation diagrams based on the parameters $\bar{g}_K$ and $\bar{g}_{Na}$. Both have an extensive region of bistability.

A bifurcation diagram based on $\bar{g}_L$ (not shown) can be made to exhibit a relatively small region of bistability by reducing the maximal potassium conductance to a value below 3 mS/cm^2. This is because with the default parameter value $\bar{g}_K = 36$ mS/cm^2 altering $\bar{g}_L$ does not provide sufficient change in the leak current, relative to the potassium current, to alter the model stability from stable to unstable. Only after drastically reducing $\bar{g}_K$ does the leak current have such an effect

with consequent unacceptable changes in resting potential, threshold and the I-V curve. Because of this finding, we do not pursue further the possibility that bursting can arise through shifting of the leak current.

Comparing the $\bar{g}_K$ and $\bar{g}_{Na}$ bifurcation diagrams (Fig. 4a, b), we see that a burster can in principle be constructed based either on the left or on the right portion of the $\bar{g}_K$ bifurcation diagram. If the right (left) portion is employed, $\bar{g}_K$ must decrease (increase) during the quiescent period, with opposite behavior during oscillations. Analogous considerations apply to the $\bar{g}_{Na}$ bifurcation diagram, taking into account that it is qualitatively a mirror image of the $\bar{g}_K$ diagram. But applying physiological constraints, only the right portion of the $\bar{g}_K$ bifurcation diagram can be used since the resting potential on the left side is above physiological values. (Similar considerations rule out the $\bar{g}_{Na}$ right portion, not shown in Fig. 4b.) The other possibility (based on the left portion of the $\bar{g}_{Na}$ diagram) will be considered below. Also see Rinzel (1987) where both possibilities (and others) are considered as part of a classification of bursting mechanisms.

To gain the maximal degree of understanding as to the principles governing bursting, we wish to examine an overall scheme for obtaining bursting. This scheme is the generation of bursts by "automatic" voltage-driven oscillations of a key parameter through a bistable region. For definiteness, we base our discussion on the qualitative features of the right portion of the bifurcation diagram in Fig. 4a.

Upon examination of the right half of the bifurcation diagram in Fig. 4a, we notice once again that in order to obtain bursting $\bar{g}_K$ must increase during oscillation and decrease during quiescence. It is important at this point not to stray from essentials in discussing which biophysical mechanisms might be responsible for the appropriate behavior of $\bar{g}_K$. To generate the required behavior of $\bar{g}_K$ in a simple manner, we thus postulate the following phenomenological equation:

$$d(\bar{g}_K)/dt = S(V)(V - V_{rest}) - d(\bar{g}_K - \bar{g}_K^{(rest)}) . \qquad (7)$$

The first term of (7) is a voltage-dependent "source" which tends to increase $\bar{g}_K$. The second term is a voltage-independent decay term, with rate of decay d. Note that when $V = V_{rest}$, $\bar{g}_K$ has the steady state value $\bar{g}_K^{(rest)}$. The choice of $\bar{g}_K^{(rest)}$ thus can place the parameter $\bar{g}_K$ in an appropriate range of values, which will determine the type of burster behavior (see below).

To decrease $\bar{g}_K$ during quiescence and to increase $\bar{g}_K$ during oscillations we postulate a source term in (7) that is relatively large during the relatively high average voltage oscillatory period. Thereby $\bar{g}_K$ increases by a certain amount during each action potential and decays between action potentials. We took $S(V) = S \cdot S_\infty(V)$, a constant source term S multiplied by $S_\infty(V) = (1 + \exp[-2a^{(s)}(V - V_{1/2}^{(s)})])^{-1}$, a sigmoid function dependent on voltage. We chose parameters so that the source is turned on only when V significantly exceeds V_{rest}. Without $S_\infty(V)$ the increase of $\bar{g}_K$ when V exceeds V_{rest} would be lost during the refractory period when the voltage is below V_{rest} so that the factor $V - V_{rest}$ in (7) is negative. The decay term was chosen such that during quiescence $\bar{g}_K$ is reduced and during oscillation $\bar{g}_K$ increases. Otherwise, if the decay term exceeds the source term, $\bar{g}_K$ would remain near its steady state value $\bar{g}_K^{(rest)}$.

3.2 Bursting behavior as determined by $\bar{g}_K$

We will show two types of bursting behaviors employing (7) together with our minimal model (1)–(6). The first type of bursting behavior is that of an *endogenous burster*. Such a burster is a cell that does not require an external input to burst and continually alternates between an oscillatory state and quiescent state (see Fig. 5a). The second type of bursting behavior is that of a *conditional burster*. This cell requires a brief external

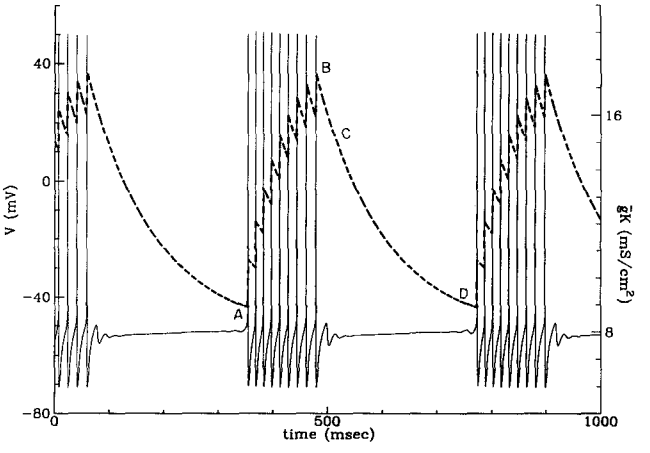

a

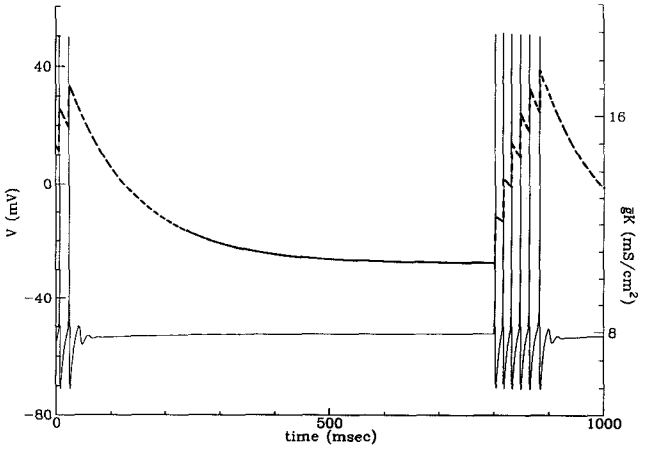

b

Fig. 5a, b. Membrane voltage (*solid line*) and $\bar{g}_K$ (*dashed line*). **a** An endogenous bursting model, based on the minimal lobster cardiac model (see Fig. 2) and (7) with $\bar{g}_K^{(rest)} = 8$. The points A–D here correspond to the like-designated points in Fig. 4a. **b** A conditional bursting model, as in **a** but $\bar{g}_K^{(rest)} = 10.6$. At *left*, the last two spikes of a burst and the subsequent approach to quiescence. The second burst was triggered by a 5 μA/cm^2 pulse at $t = 800$ ms for 0.5 ms. Model parameters (1)–(6) as in Fig. 2. Parameters of (7): $S = 0.04$, $V_{1/2}^{(s)} = -20$ mV, $a^{(s)} = 0.2$, $V_{rest} = -56$ mV, $d = 0.008$

input to enter its oscillatory state. After firing several action potentials the cell will return to its quiescent state, where it will remain until further input. Merely by changing $\bar{g}_K^{(rest)}$, a conditional burster can be obtained, as shown in Fig. 5b.

We now wish to dissect the bursting behavior, by means of the bifurcation diagram. To aid in this effort we have superimposed a closed heavy line on the bifurcation diagram of Fig. 4a. Traversal of this line in the direction of the arrow schematically indicates the time course of $\bar{g}_K$, and of solution behavior during a brust. Letters A–D in Fig. 4a are placed to refer to corresponding points in Fig. 5a.

Let us first discuss the time course of a burst in broad terms (leaving certain discrepancies between Fig. 4a and Fig. 5a to be explained later). We start at A in Fig. 4a, where it is seen that $\bar{g}_K$ is at its minimum value among all points on the heavy line. Oscillations commence (see Fig. 5a). (Note that in Fig. 4a the presence of oscillations is symbolized by placing the heavy line close to the point that corresponds to the minimum voltage during the oscillation.) The oscillations induce an increase in $\bar{g}_K$ into a region wherein oscillations are no longer possible; thus at point B oscillations cease. As seen in Fig. 4a there is a transition to C, a steady (quiescent state). During quiescence, $\bar{g}_K$ decreases until it drops into a region where the steady state is no longer stable. Indeed, the system moves from a quiescent state at D to oscillations at A.

There are certain differences between the behavior expected from the bifurcation diagram of Fig. 4a and the actual behavior observed in the simulations of Fig. 5a. For example, according to Fig. 4a, oscillations should cease when $\bar{g}_K$ exceeds 16.3, while according to Fig. 5a the oscillations actually terminate when $\bar{g}_K$ exceeds 17. This seeming discrepancy occurs because the schematic heavy line in Fig. 4a does not indicate that the progress of $\bar{g}_K$ is not monotonic, but oscillatory. In the penultimate spike of a burst, $\bar{g}_K$ briefly exceeds the critical value 16.3 above which oscillations become extinguished. But before the "extinction process" has time to take place, $\bar{g}_K$ has dropped below 16.3. During the next spike, however, $\bar{g}_K$ remains above 16.3 for long enough to induce extinction of the oscillations.

Another discrepancy is that in Fig. 5a quiescence continues to point D, while according to Fig. 4a oscillations should commence earlier, when $\bar{g}_K$ drops below 10. The reason for this behavior follows from the observation that oscillations inevitably develop if $\bar{g}_K$ is held at a fixed value slightly below 10, but simulations show that it takes on the order of 3000 ms for the oscillations to appear. Thus oscillations indeed start developing when expected, but so slowly that no effect can be discerned in Fig. 5a until $\bar{g}_K$ has dropped well below 10.

We emphasize that the present model for bursting is based upon the existence of a bistable region. This can be seen by looking once again at the heavy closed curve in Fig. 4a. As we have seen, when the conductivity drops below $\bar{g}_K = 10.5$ then the steady (quiescent) state ceases to be stable, so that the system moves toward an oscillatory state. The ensuing oscillations bring about an increase in $\bar{g}_K$, which soon exceeds the value of 10.5. Because of the existence of bistability, the system does not return to quiescence. Quiescence is indeed a stable steady state when $\bar{g}_K$ exceeds 10.5, but so is oscillatory behavior. Because the system is in (or very near) an oscillatory state when $\bar{g}_K$ exceeds 10.5 it will remain in this state – for to attain a quiescence state the system must begin in the domain of attraction of that state. A similar argument describes what occurs in transitions of $\bar{g}_K$ above and below 16, the value at which there is a change in the stability of the oscillatory state.

Figure 5b shows a conditional bursting behavior and the corresponding change in $\bar{g}_K$. To achieve this behavior we merely altered the value of $\bar{g}_K^{(rest)}$ in (7) so that the steady state value of $\bar{g}_K$ now resides within the bistable region (see Figs. 3, 4a). A burst is initiated by ensuring that $\bar{g}_k$ is in the bistable range and by supplying a suitable initial condition. During the burst the variable $\bar{g}_K$ increases, to $\bar{g}_K > 16.3$, which halts the oscillations, and then begins to decrease until it reaches the value set by $\bar{g}_K^{(rest)}$, in this case $\bar{g}_K = 10.6$. The model stays at this steady state and only an external input will shift the system into an oscillatory state.

In the remainder of this article, we shall deal only with endogenous bursters.

3.3 Biophysical processes for varying $\bar{g}_K$

We have shown that suitable alteration of the parameter $\bar{g}_K$ in the minimal excitatory–oscillatory model of paper I can provide bursting. Since $\bar{g}_K$ quantitates the maximal potassium conductance, $\bar{g}_K$ can be altered by changing the channel density. But it seems quite unreasonable that with each action potential the number of channels changes. From a broader perspective, however, changes in $\bar{g}_K$ achieve their effect by modifying the total potassium conductance $g_K^{(total)}/\bar{g}_K \equiv (W/s)^4$. We thus ask what other biophysical processes might modify $g_k^{(total)}$. There is evidence of the existence of calcium-dependent potassium channels that play a role in cell bursting (for example Hille 1992; Schwarz and Passow 1983). We have therefore chosen to incorporate a calcium-dependent potassium channel to produce a biophysically plausible bursting model.

With the incorporation of a new potassium channel, the total potassium conductance $g_K^{(total)}$ is obtained by summing the contributions from the original potassium channels and the newly postulated calcium-dependent potassium channels. The required modification of $g_K^{(total)}$ is implemented by an increase in intracellular calcium, mainly during spikes, and continuous calcium removal between spikes. Thus, to the two model equations (1) and (2) for the voltage V and the recovery variable W, we now add a third equation for the calcium concentration C.

We use calcium to activate the calcium-dependent potassium channels and therefore are only interested in the intracellular calcium concentration. The essence of our assumption concerning calcium is that its entry is

via a channel that both opens and closes on the time scale of an action potential, for this implements the discrete increase of $\bar{g}_K$ [in (7)] during each action potential. As at present we are investigating a calcium channel that possesses the same time course as the sodium channel, we assume for simplicity that during the spike calcium enters via the sodium channels. Such an assumption bypasses the necessity to add equations to describe independent calcium channels. We thereby adhere to our policy of keeping the number of processes to a minimum and of adding complexity only when required. No change in our results is anticipated if we postulate separate fast calcium channels (see below).

We thus introduce a new variable to describe the intracellular calcium concentration that is used to control the calcium-dependent potassium channels. The increase in corresponding current $I_{K(Ca)}$ will halt the oscillations. Upon the removal of calcium, oscillations will resume. The calcium-dependent potassium current $I_{K(Ca)}$ is described, following Plant (1978), as the product of the maximal conductance $\bar{g}_{K(ca)}$, a saturating function of intracellular calcium $C/(C+K_d)$ to describe the fraction of maximal conductance, and the driving force $(V-V_K)$:

$$I_{K(Ca)} = \bar{g}_{K(Ca)}\left[\frac{C}{K_d + C}\right](V - V_K) \tag{8}$$

The calcium enters via the sodium channels, so that, paralleling (3a),

$$I_{Ca} = \bar{g}_{Ca} m_\infty^3(V)(1 - W)(V - V_{Ca}) \tag{9}$$

The internal calcium concentration is modeled by

$$dC/dt = Kp(-I_{Ca}) - R \cdot C \tag{10}$$

where R is the removal rate constant and K_p is a conversion factor from current to concentration. We denote this model [(1)–(6) and (8)–(10)] the *minimal bursting model.* Note that with (8) the total potassium conductance is given by

$$g_K^{(total)} = \bar{g}_K(W/s)^4 + \bar{g}_{K(Ca)} \cdot C/(C + K_d)$$

The conductances $\bar{g}_K$ and $\bar{g}_{K(Ca)}$ are determined so as to retain the fundamental idea of our bursting model, that potassium conductance traverses a region of bistability.

Calcium is incorporated into our model solely for its effect on the Ca-dependent potassium channels; the calcium current is important only as a means for regulating the intracellular calcium concentration. Thus we choose the parameters, $\bar{g}_{Ca}$, K_p and R in (10) so that there is a reasonable $[Ca]_i$ at rest [0.05 μM in our model; 0.02–0.3 μM according to Hille (1992)] and so that calcium increases sufficiently above rest to suitably affect the total potassium conductance.

3.4 Properties of the minimal bursting model

Figure 6 shows the bursting behavior obtained with our present model [(1)–(6) and (8)–(10)]. We note that, as expected, the results correspond to those obtained using (7) (see Fig. 5a). The oscillatory behavior depicted in Fig. 6 (top) corresponds to the period of increasing

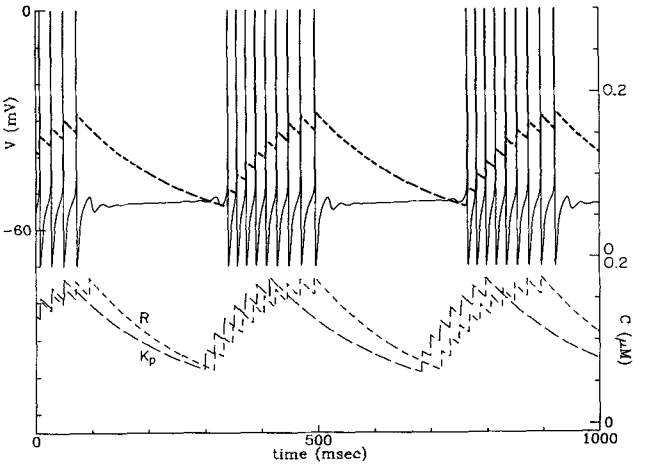

Fig. 6. The minimal bursting model based on the minimal lobster cardiac model (see **Fig. 2**). *Top*: Membrane voltage (*solid line*) and intracellular calcium concentration (*dashed line*). *Bottom*: The effect on intracellular calcium concentration of a 10% increase in calcium removal R (*short-dashed line*) and calcium influx K_p (*long-dashed line*). Model parameters (1)–(6) as in Fig. 2 with $\bar{g}_K = 8$ mS/cm^2. Parameters of (8)–(10): $\bar{g}_{K(Ca)} = 0.25$ mS/cm^2, $K_d = 0.5$, $\bar{g}_{Ca} = 5$ mS/cm^2, $V_{Ca} = 124$ mV, $K_p = 0.00052$, $R = 0.0045$

intracellular calcium until a threshold is attained where the oscillation is halted. Calcium is removed during the quiescent period, until oscillations resume.

To examine the properties of the minimal bursting model we note that there are three primary features that characterize a burster: the duration of the oscillatory period (T_{osc}), the duration of the quiescent period (T_{qui}) and the frequency (f) of the oscillation. Of course $T_{osc} + T_{qui} = T$ where T is the period of the burster. It is natural to inquire which of the model parameters strongly affects each of these features. T_{qui} should be principally affected by the removal parameter R that governs the speed at which C decreases. T_{osc} should depend primarily on the amount by which C increases during each spike, that is, primarily on the calcium influx parameter K_p [see (10)]. Figure 6 (bottom) demonstrates that R and K_p indeed have the expected effects. A 10% increase in the removal parameter R leads to a decrease in the quiescent duration from 270 ms to 225 ms as well as increasing the oscillations by 25 ms and one action potential. A similar increase in calcium influx K_p reduces the burst duration and number of action potentials from 155 ms with nine spikes to 115 ms with seven spikes; the quiescence duration is unaltered.

Of course, similar modifications of T_{osc} and T_{qui} can be obtained by changing the corresponding parameters d and S of (7) (not shown). Therefore the variation of the source term in the $\bar{g}_K$ equation (or its biophysical implementation) alters T_{ocs}, while variation of the decay term (or its biophysical implementation) alters T_{qui}.

Significant alteration of the frequency f can only be accomplished by changing the parameters in the minimal cell model of paper I. Indeed, in paper I we studied the influence of parameters and concluded that alterations in $\bar{g}_K$, V_K and input current I could influence the

frequency of oscillation. Only very large changes in $\bar{g}_K$ would cause any appreciable frequency change, (and an undesired by-product of this change would be alterations in the qualitative behavior of the system). The same applies to V_K, since the resting potential shifts by 10 mV for every two-fold change in concentration. The input current variable was found to be most suitable for frequency alteration, and this direction will be pursued.

4 A basic bursting model

4.1 An inward current

The minimal bursting model described above includes parameters that control burst duration, the length of the oscillatory and quiescent periods. However, the third major feature of bursts, the frequency of firing during the burst, is fixed. Moreover, based on the model in paper I we find the input current to be the most suitable variable for altering frequency. Since, for other reasons, calcium has already been introduced in the minimal bursting model we will use calcium for our input current. Recall that in the minimal bursting model calcium entered via a fast channel during the action potential. As the peak I_{Ca} is less than 10% of the peak I_{Na}, the calcium current played a negligible role in the currents that contributed to the system dynamics. For I_{Ca} to have a significant effect, it is not sufficient for calcium ions to flow through channels that remain open only for the extent of an action potential, such as the sodium channels that were used for simplicity above. A new slow calcium channel has to be introduced to allow a flow of calcium for a time much longer than the duration of an action potential. Then the inward calcium flow will act as an inward current and cause an alteration of the firing frequency. We describe the new calcium current as

$$I_{Ca} = \bar{g}_{Ca} \cdot X \cdot (V - V_{Ca}) \tag{11}$$

similarly to our other currents. Paralleling (2) and (4) we assume

$$dX/dt = (X_\infty(V) - X)/\tau_x \quad \text{with} \quad X_\infty(V)$$
$$X_\infty(V) = (1 + \exp[-2a^{(x)}(V - V_{1/2}^{(x)})])^{-1} \tag{12}$$

where τ_x is taken to be constant. We denote this model [(1)–(6), (8) and (10)–(12)] the *basic bursting model.*

The parameters of the calcium activation variable X will be discussed in the following section.

4.2 Effects of calcium activation

The role of the variable X is to keep the calcium channels open for a long period of time, between the action potentials. This allows for a constant calcium flow of a long duration. Therefore, even though the maximal calcium conductance is small in comparison to the maximal sodium conductance, the calcium flow that occurs between action potentials (when very little sodium flows) greatly increases the importance of this inward current. As a consequence, changing the value of the calcium conductivity $\bar{g}_{Ca} \cdot X$ is a means of altering the inward current and thereby the level of depolarization for the duration of the calcium flow, which alters the firing frequency during the burst.

We first confirm that if τ_x is of a short duration, e.g. 1 ms, i.e. the same time scale as that of an action potential, we achieve the same behavior as was previously shown (see Fig. 6 (top)) when the calcium flowed through the sodium channels. To this end the parameters of the activation variable X, $V_{1/2}^{(x)}$ and $a^{(x)}$, were chosen so that the influx of calcium corresponds to the previous results of the minimal bursting model. Figure 7a shows the membrane potential V, intracellular calcium C and X variable for the resulting burster (with $\tau_x = 1$). The burst cycle is similar to that of the minimal burster in durations (T_{osc} and T_{qui}) and frequency.

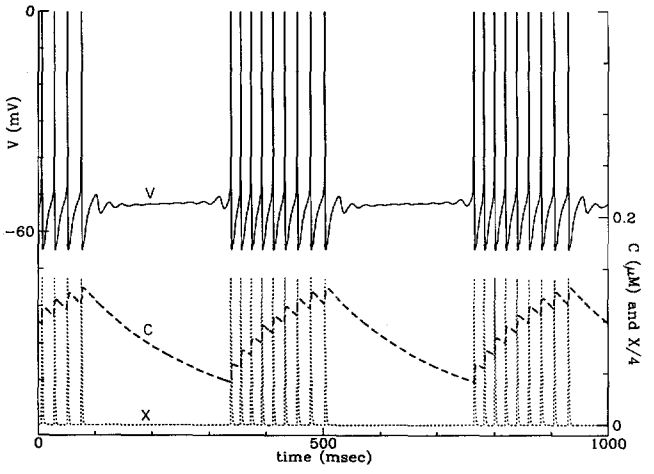

a

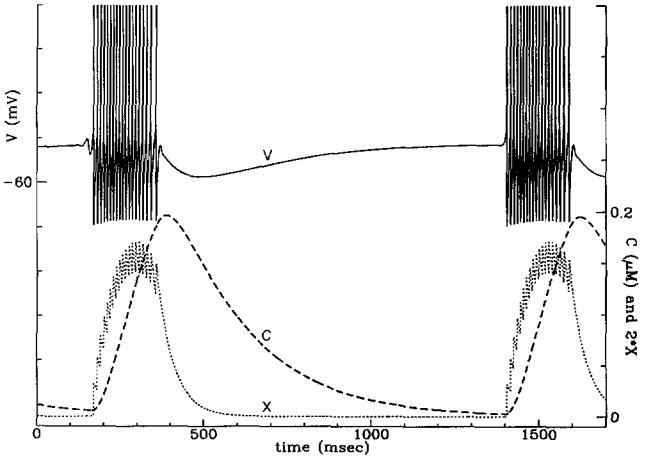

b

Fig. 7a, b. Bursting behavior for basic model. Membrane potential V (*solid line*), intracellular calcium concentration C (*long-dashed line*) and calcium activation variable X (*short-dashed line*). **a** X variable relaxation time $\tau_x = 1$ ms. **b** X variable relaxation time $\tau_x = 50$ ms and $\bar{g}_{K(Ca)} = 1$ mS/cm^2. Model parameters (1)–(6) as in Fig. 2 with $\bar{g}_K = 8$ mS/cm^2. Parameters of (8), (10)–(12): $\bar{g}_{K(Ca)} = 0.25$ mS/cm^2, $K_d = 0.5$, $\bar{g}_{Ca} = 0.5$ mS/cm^2, $V_{Ca} = 124$ mV, $K_p = 0.00025$, $R = 0.0045$, $V_{1/2}^{(x)} = -20$ mV, $a^{(x)} = 0.2$

Table 1. Comparison of basic model for altered τ_x and $\bar{g}_{Ca}$

$\bar{g}_{Ca}$ (mS/cm^2)	τ_x (ms)	Burst period (ms)	T_{osc} (ms)	T_{qui} (ms)	Peak f (Hz)
0.5	1	425	165	260	57
0.5	50	1235	185	1050	110
1.0	50	1540	260	1280	139

We now show the role of X in keeping the calcium channels open for a long period. Figure 7b shows a bursting model with $\tau_x = 50$ ms (cf. Fig 7a). Table 1 compares the salient features of the two bursting models, with a calcium activation variable that is fast ($\tau_x = 1$ as in the minimal bursting model) and slow ($\tau_x = 50$; basic model). Once a slow current has been created, its magnitude becomes influential. In particular (as is also illustrated in Table 1) by increasing $\bar{g}_{Ca}$ we achieve a somewhat higher frequency and period of oscillation. This is caused by a larger calcium current which also extends the burst period, both with a longer T_{osc} and with an extended T_{qui}.

A comparison of Fig. 7a and Fig. 7b shows that with a longer relaxation time, $\tau_x = 50$ ms, the change of intracellular calcium is greatly altered. The range of $[Ca]_i$, from its peak (at the end of the oscillations) to its minimum (just before oscillations) is large, over a 50-fold change in magnitude. This compares with a three-fold change with $\tau_x = 1$ ms.

The change in the activation variable X shows the direct effect of the altered relaxation time. In Fig. 7b X is active for the duration of the burst, although the peak activation with the long relaxation time is much lower than for the fast relaxation case. Indeed, the slow relaxation time causes the X variable to increase slowly and stay high for a long time, in comparison with the time scale of an action potential.

5 Bursting behavior as determined by $\bar{g}_{Na}$

Our preceding development of a basic bursting model was based on a minimal burster that alters the total potassium conductance. It follows from Fig. 4b that the sodium conductance $\bar{g}_{Na}$ could also be a suitable parameter for achieving bursting using (1)–(6) and (7) with $\bar{g}_K$ replaced by a suitable equation inolving $\bar{g}_{Na}$. Based on Fig. 4b, we would like $\bar{g}_{Na}$ to incease during quiescence and decrease during oscillation. To that end we have to reverse the leading signs of the terms in (7); the term sensitive to voltage should now reduce $\bar{g}_{Na}$, and the term that brings about the steady-state value of $\bar{g}_{Na}$ should increase $\bar{g}_{Na}$. With this alteration of roles, we achieve a burster using (1)–(6) and a modified (7) (not shown).

5.1 A biophysical alteration of $\bar{g}_{Na}$

We do not know of a process that increases sodium flow during quiescence and decreases its flow during oscillation. A process that could play such a role is an inward current (or leak) with calcium-dependent inactivation. If we identify the "control parameter" for bursting with the total inward currents, then we can incorporate a new current that will change its maximal flow during the course of a burst cycle. This can mimic the desired behavior of $\bar{g}_{Na}$ in Fig. 4b. When the total maximal inward conductance, denoted by $g_{Na}^{(total)}$, is low $g_{Na}^{(total)} < 113$ mS/cm^2, the system possesses a globally stable steady state. This is the result of a high intracellular calcium level, which will cause strong inactivation of the "new" inward channels. As calcium is removed during quiescence, the inactivation will decrease and thereby allow an increase of inward conductance. During this increase in conductance the bistable region will be traversed with the membrane voltage as its steady state. Eventually, the system will reach a sufficiently high inward conductance ($g_{Na}^{(total)} > 155$ mS/cm^2) so that the steady state becomes unstable (see Fig. 4b) and the system will begin to oscillate. During the oscillation the bistable region will be traversed again. Calcium will enter and increase the Ca-dependent inactivation. Upon sufficient inactivation the inward conductance will decrease such that the steady state is globally stable and oscillations will halt.

Such behavior can be described by adding one process to the minimal model of paper I [(1)–(6)]. An inward current or leak, which is inactivated as intracellular calcium increases, will bring about the behavior described above. This will be similar to the minimal bursting model presented earlier. The duration of oscillations and quiesence can be altered by modifying model parameters, following the arguments presented previously. To alter the frequency of firing, we can repeat the previous procedure by incorporating a calcium channel with an activation variable X of a long time scale in comparison with the duration of an action potential. We will not implement the above model, but merely note that it is possible to achieve a basic model using the inward conductance as a cyclic variable for bursting.

6 Summary and discussion

In our study of bursting we took a two-pronged approach, gaining understanding independent of specific mechanisms and only then suggesting and examining mechanisms that are at once biophysically reasonable and of minimal complexity. We have shown that the minimal cell model of paper I can be extended to produce bursting behavior. The bursting mechanism that we have employed depends on the existence of a bistable region for some parameter domain. By incorporating a process that alters the conductance of any of the three currents that play a role in the nerve model, a minimal bursting model can in principle be designed.

Choosing potassium as the "control current" we implemented a bursting model, using a biophysically known process, a calcium-dependent potassium channel, to alter the total potassium conductance during the burst cycle.

With such a bursting model one can alter the duration of oscillation and the duration of quiescence, but not the oscillation frequency. To achieve a burster model that can in addition show different frequencies of oscillation an additional process was needed, namely an inward current. We implemented this requirement by introducing calcium channels that remain open long after the classical sodium channels close. In this manner we can alter the calcium influx during the oscillation period and have a background depolarization of different intensities, depending on $\bar{g}_{Ca}$. The possibility of altering the calcium current allows for different frequencies of oscillation.

We have indicated that altering the maximal sodium conductance can also provide a bursting mechanism. This possibility seems biophysically more difficult to implement, as it requires that the total inward conductance should increase during quiescence and decrease during oscillation. One possibility is for a new inward leak (or current) that has calcium-dependent inactivation to provide for the change in conductance. In addition, some process for altering the frequency of oscillation is needed, but this could be implemented in the same way as for the $\bar{g}_K$-dependent bursting model. One possible candidate for the inward current is a calcium current. It is known that some calcium channels have calcium-dependent inactivation and play a role in bursting neurons (Hille 1992). Indeed, Rinzel and Lee (1987) have presented a bursting model using calcium inactivation of a calcium conductance.

The next step in our program will be to model the behavior of our "case study" neurons, the lobster cardiac ganglion cells. These cells show different bursting characteristics, in terms of the burst cycle, both oscillation and quiescence durations, as well as firing frequencies. The cells seen in the ganglion are either endogenous bursters, conditional bursters or follower cells. The results of paper I and this paper provide us with the means to model these cells by a single basic model whose parameters can be altered in a quest to provide the observed behavior.

References

Av-Ron E, Parnas H, Segel LA (1991) A minimal biophysical model for an excitable and oscillatory neuron. Biol Cybern 65:487–500

Bullock TH, Terzuolo CA (1957) Diverse forms of activity in the somata of spontaneous and integrating ganglion cells. J Physiol (Lond) 138:341–364

FitzHugh R (1961) Impulses and physiological states in theoretical models of nerve membrane. Biophys J 1:445–466

Hille B (1992) Ionic channels of excitable membranes (Second edition). Sinauer, Inc., Sunderland, Mass

Hodgkin AL, Huxley AF (1952) A quantitative description of membrane current and its application to conduction and excitation in nerve. J Physiol (Lond) 117:500–544

Otani T, Bullock TH (1959) Effects of presetting the membrane potential of the soma of spontaneous and integrating ganglion cells. Physiol Zool 32:104–114

Plant RE (1978) The effects of calcium^{2+} on bursting neurons. Biophys J 21:217–237

Rinzel J (1984) Excitation dynamics: insights from simplified membrane models. Proceedings of 68th Annual Meeting of Federation of American Societies for Experimental Biology, St Louis, Mo

Rinzel J (1987) A formal classification of bursting mechanisms in excitable systems. In: Teramoto E, Yamaguti M (eds) Mathematical topics in population biology, morphogenesis and neurosciences. (Lecture notes in biomathematics, vol 71) Springer, Heidelberg New York, pp 267–281

Rinzel J, Lee YS (1987) Dissection of a model for neuronal parabolic bursting. J. Math Biol 25:653–675

Rinzel J, Ermentrout GB (1989) Analysis of neural excitability and oscillations. In: Koch C, Segev I (eds) Methods in neuronal modeling: from synapses to networks. MIT Press, Bradford, Mass

Schwarz W, Passow H (1983) Ca^{2+}-activated K^+ channels in erythrocytes and excitable cells. Annu Rev Physiol 45:359–357